Journal of Polymers and the Environment (2023) 31:238–248
https://doi.org/10.1007/s10924-022-02603-1

ORIGINAL PAPER

Affinity Polymer Membrane Containing Nitrilotriacetic Acid, Ethylene Diamine Tetra Acetic Acid and Tris (2-Aminoethyl) Amine as Carriers for the Recovery of Nickel (II) from Acidic Industrial Discharges

Z. Habibi[1] · O. Kamal[1] · M. Riri[1] · Y. Chaouqi[2] · K. Touaj[1] · S. Majid[1] · L. Lebrun[3] · M. Hlaibi[1,3]

Accepted: 21 September 2022 / Published online: 27 October 2022

Abstract

In the present work, we prepared three polymer inclusion membranes (PIM), based on polyvinyl alcohol (PVA) as polymeric support and containing three extractive agents: Nitrilotriacetic acid (NTA), Ethylene diamine tetra acetic acid (EDTA) and tris (2-aminoethyl) amine (TREN). The morphology structures of these membranes were determined using different spectroscopical techniques by Fourier-transform infrared spectrometry and scanning electron microscopy techniques. The membranes were used to conduct experiments of oriented extraction processes for the facilitated recovery of Nickel (II) ions from lithium-ion (Li-ion) battery waste. The obtained results allowed to determine the values of different macroscopic and microscopic parameters of paramount importance such as respective permeability ($\boldsymbol{P}$), initial flux ($\boldsymbol{J_0}$) and apparent diffusion coefficient ($\boldsymbol{D^*}$), constant association ($\boldsymbol{K_{ass}}$) related to the movement of the substrate through the membrane. The influence of several factors, as the initial substrate concentration and temperature ($\mathbf{C_0}$, $\mathbf{T}$) was studied. The results indicate that the different parameters ($\boldsymbol{P}$, $\boldsymbol{J_0}$, $\boldsymbol{D^*}$ and $\boldsymbol{K_{ass}}$) vary strongly with the temperature of the medium and that of the performances of the used membranes increase with the temperature factor. The activation and thermodynamic parameters ($\boldsymbol{E_a}$, $\boldsymbol{\Delta H^{\#}_{ass}}$ and $\boldsymbol{\Delta S^{\#}}$, $\Delta \boldsymbol{H_{th}}$ **and** $\Delta \boldsymbol{H_{diss}}^{\#}$) were also determined and their values indicate a kinetic control for the mechanism of the studied processes, which explains the high performances of the developed membranes and indicates a mechanism by successive jumps of Nickel (II) ions on fixed sites of the extractive carriers immobilized in the membrane phase.

Keywords Extractive agents · Polymer inclusion membranes · Recovery of Nickel (II) ions · Li-ion battery waste

Introduction

Li-ion battery waste are electronic product waste containing large amounts of key raw materials such as cobalt, lithium, manganese and nickel, as well as hazardous substances [1–5]. On one hand. If lithium-ion (Li-ion) battery waste is not properly managed, these valuable metals and toxic substances end up in the environment and cause environmental and public health issues [6–8]. Effective management and recycling of dead Li-ion batteries is critical to protect nature, ensure sustainable resource management and stimulate a circular economy [9–11]. On the other hand, more conventional methods using a combination of pyrometallurgic treatment with hydrometallurgical processing have been widely studied to recover metals from Li-ion battery waste [12–16]. Also there are other methods for the recovery of these metals from industrial waste such as liquid–liquid extraction [17, 18], chemical precipitation [19], adsorption on activated carbon [20, 21], ion exchange on resins[22], and membrane process techniques [23–27]. Membrane processes have advantages over other conventional techniques, such as good selectivity, lack of phase change during separation operations, modularity and low consumption of energy compared to other processes [28]. These membranes techniques are based on the properties of a semi-permeable barrier working under

✉ Z. Habibi
habibizakaria18.32@gmail.com

✉ M. Hlaibi
m.hlaibi.58@gmail.com

[1] Laboratory of Materials Engineering for Environment and Valorization (GeMEV), Faculty of Sciences Ain-Chock, University Hassan II, Casablanca, Morocco

[2] Laboratory of Research on Textile Materials (REMTEX), ESITH Casablanca, Casablanca, Morocco

[3] Laboratory of Polymers, Biopolymers, Surfaces (PBS), CNRS UMR 6270, Faculty of Science and Technology, 76821 Mont-Saint-Aignan, France

the effect of a transfer force, thus allowing certain molecules to pass selectively and to retain others [29].

In this present study, we focused on the use of polymer inclusion membranes (PIM) which consist of a polymer supports, polyvinyl alcohol (PVA) containing three types of extractive agents Nitrilotriacetic acid (NTA), ethylenediaminetetraacetic acid (EDTA) and tris (2-aminoethyl) amine (TREN) (Fig. 1). In order to quantify the performances of the elaborated PIM, we determined the macroscopic parameters, the membrane permeability $\boldsymbol{P}$ and the initial flux $\boldsymbol{J_0}$, and the microscopic parameters, the constant association $\boldsymbol{K_{ass}}$ and the apparent diffusion coefficient $\boldsymbol{D^*}$ obtained from the Fick's first law. Moreover, to explain the substrate process of extractions and recovery of Nickel (II) ions from Li-ion battery waste by the elaborated membranes, and to elucidate its mechanistic aspects, the activation energy $\boldsymbol{E_a}$, the association enthalpy $\boldsymbol{\Delta H^{\neq}}$ and the entropy $\boldsymbol{\Delta S^{\neq}}$, the thermodynamic enthalpy ($\boldsymbol{\Delta H_{th}}$) and dissociation enthalpy ($\boldsymbol{\Delta H^{\neq}_{diss}}$) were determined and the obtained results show that the suggested orientation process takes place due to successive jumps.

Therefore, these energetic values can be used to explain the performance of the used membranes and elucidate the energetic and structural kinetic aspects that control the mechanisms of oriented processes through the PIM membrane.

Materials and Methods

Calculations

The permeability $\boldsymbol{P}$ and the initial flux $\boldsymbol{J_0}$ are determined from the following equations [30–32]:

$$P\,(t - tL) = (\ell^{*}V/2^{*}S)\,Ln\left(C_0/\,C_0 - 2C_R\right) \tag{1}$$

$$P\;=\;a^{*}V^{*}\ell/2^{*}S \text{ and } J_0 = P^{*}\,C_0/\ell \tag{2}$$

a: the slope value of the linear representation of $-Ln(C_0-2Cr) = f(t)$. ℓ: the membrane thickness. S: the active surface of the barrier membrane in contact with the aqueous solutions. V: the volume of the receiving phase.

$\boldsymbol{K_{ass}}$ and $\boldsymbol{D^*}$ are calculated by the following equation:

$$1/\,J_0 = 1/\,D^{*}\left(\left(1/[T]_0\,^{*}K_{ass}\,^{*}C_0\right) + 1/[T]_0\right) \tag{3}$$

$$K_{ass} = \frac{\text{intercept (o.o)}}{\text{slope (p)}}$$

$$D^{*} = \left(\frac{1}{o.o}\right)*\left(1/[T]_0\right) \tag{4}$$

where p are the values of the experimental line slope and O.O the intercept of $1/J_0 = f(1/C_0)$. $[T]_0$: the total and fixed concentrate of the extractive agent in the membrane phase.

The initial flux is related to the temperature, according to the Arrhenius law by the follow equation:

$$J(T) = \;AjExp\left(-E_a/RT\right) \tag{5}$$

$\boldsymbol{R}$: Ideal gas constant, $\boldsymbol{A_j}$: pre-exponential factor, $\boldsymbol{E_a}$: activation energy for the transition state of the kinetically determining step which is the diffusion of the substrate S through the membrane by the intermediate entity (ST).

After linearization we have the following relation

$$LnJ_0 = \;-\,E_a/R \times (1/T) + \;lnAj \tag{6}$$

The value of $\boldsymbol{E_a}$ parameter is determined from the slope of the line segment $\ln(J_0) = f(1/T)$. It is known from the activated complex theory that $\boldsymbol{E_a}$ is related to the activation enthalpy parameter $\boldsymbol{\Delta H^{\#}_{ass}}$ as follows:

$$\mathbf{\Delta Hass^{\#}} \;=\; \mathbf{Ea} - 2500\text{ J mol} \;-\; 1\;\mathbf{at}\;298\text{ K} \tag{7}$$

While the entropy parameter $\boldsymbol{\Delta S^{\#}}$ is related to the pre-exponential factor by the relation:

$$\Delta S^{\#} \;=\; R\,(LnAj - 30,46)\text{ J mol}^{-1}\text{ at }298\text{ K} \tag{8}$$

Elucidation and quantification of energy and/or kinetic pathways associated with Nickel (II) ions are carefully designed membrane. The value of $\boldsymbol{\Delta H_{th}}$, which is the enthalpy of equilibrium substrate S and the extractive agent T in the membrane phase was determined. Integral of Van't Hoff's law ($dLn\boldsymbol{K_{ass}}/dT = \boldsymbol{\Delta H_{th}}/RT^2$) expresses the evolution of the associated constant parameter ($\boldsymbol{K_{ass}}$) as Temperature.

$$Ln(Kass) = -\Delta Hth/RT + cste \tag{9}$$

The slope of the linear representation $Ln(\boldsymbol{K_{ass}}) = f(1/T)$ allows to determine the value of the $\boldsymbol{\Delta H_{th}}$ related to the

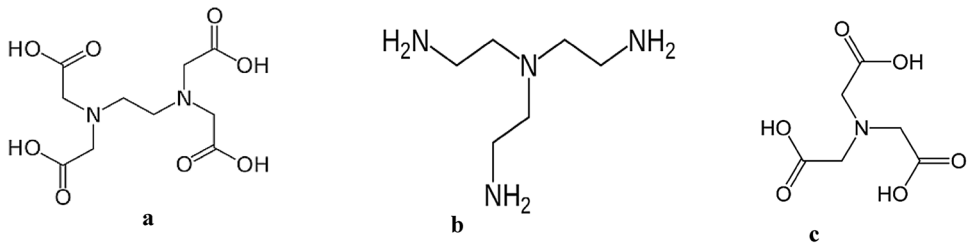

Fig. 1 Structure of extractive agents; **a** EDTA, **b** TREN, **c** NTA

activation parameters ($\Delta H^{\#}_{ass}$ and $\Delta H^{\#}_{diss}$) which is based on following expression.

$$\Delta Hth = \Delta H\#ass - \Delta H\#dis \quad (10)$$

Chemicals

All chemicals, reagents and solvents were pure commercial products of analytical grade (Aldrich, Fluka). The polymer support used PVA was supplied by (Loba Chemie).

Extraction experiments

The double cell used to carry out the experiments of the facilitated transport of Nickel (II) ions consists of two glass compartments separated by the examined membrane. A compartment containing the feed phase of Nickel (II) ions at the examined concentration and a compartment containing the receiving phase consisting of distilled water. The system is immersed in a thermostat bath containing water in order to keep the temperature constant throughout the experiments. A multi-position stirrer is used to ensure the homogeneity of the two phases [33–35]. Micro volumes samples were taken from the feed phase at regular time intervals and analyzed by a Mettler Toledo UV–visible spectrophotometry device.

Preparation of the PIM membranes:

The preparation of the membranes consists of mixing 10 g of PVA with 20 ml of Dimethylsulfoxide (DMSO) and 80 ml of distilled water (DE) as solvent in a tightly closed bottle to prevent evaporation. The mixture is stirred for 24 h at a temperature of 393 K to solubilize the PVA in the solution. To this solution we added 0.5 g of transporter (NTA, EDTA and TREN). The whole mixture is stirred for 6 h at 333 K, using a hot plate. Finally, we casted the membrane into a Petri dish and then put it in an oven at 338 K to dry. The following notations were adopted for the prepared PIM membranes. We used a Mitutoyo Palmer electronic device, with an accuracy of 0.001 mm for the measurement of the thickness of the obtained membranes is determined by performing an average calculation on the values measured in twelve different places and we found E (PVA-NTA) = 0.102 mm, E(PVA-EDTA) = 0.15 mm and E(PVA-TREN) = 0.17 mm.

Results and discussion

Characterization of the developed membranes by FTIR

Analysis by the (Fourier-Transform Infrared Spectroscopy) FTIR spectrometric technique (Fig. 2) was used to study and identify the functional groups of the PIM membranes that were developed. The PVA polymer support membrane alone

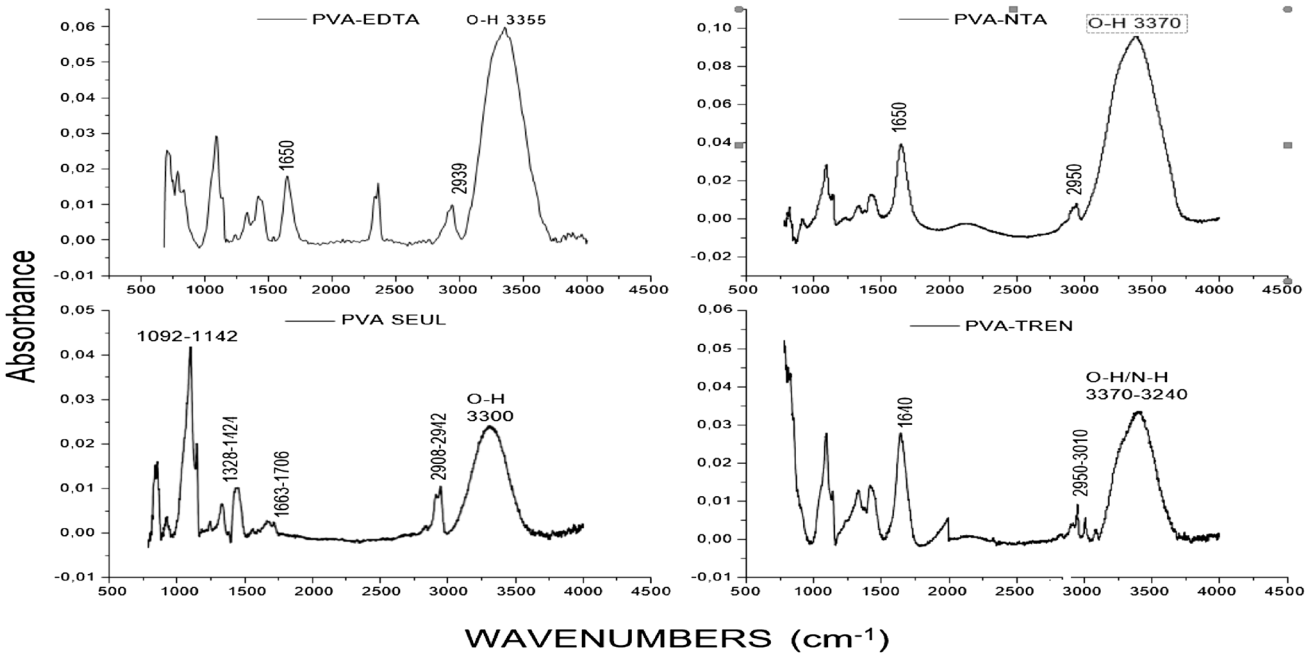

Fig. 2 FTIR spectra relative to the different constituents of the developed PIMs membranes: *PVA/ NTA-EDTA-TREN*

and the other membranes prepared from the PVA support and the various extractive agents NTA, EDTA, TREN with 6% (w/w) of the total polymer membrane mass. The characteristic peaks typical of the PVA support located between 3100 and 3500 and at 1707 cm^{-1} related respectively to the stretching vibrations of the bound O–H bonds, and to the stretching vibrations of the C=O bonds of the acetate group present after the production of PVA from the hydrolysis of the polymer and its dehydration [36]. Nevertheless, the peak at 3100–3500 cm^{-1} of membranes containing NTA and EDTA is more intense due to the inclusion of O–H functions between the PVA chains. While it is observed that there is a change in the shape of the peak towards at 3240–3370 cm^{-1} in the membrane containing the TREN agent compared to that of stretching of the hydroxyl groups in the spectrum of the PVA support. The bands at 1093, 1420 and 2941 cm^{-1} are respectively attributed to the stretching vibrations of the C–O, C–H bonds of the PVA. After the inclusion of each of the carriers in the polymeric support, a new peak was detected at 1650 cm^{-1} in the spectra of the PVA-NTA and PVA-EDTA membrane, which was attributed to the vibration of the carboxylic group C=O and in the spectrum of the PVA-TREN membrane, the vibration bands of the NH2 groups can be observed at 1640 cm^{-1} which corresponds to the deformation of the N–H bond (primary amine). A new peak at 3010 cm^{-1} appears in the TREN-modified PVA membrane, which is probably attributed to stretching vibrations of the –CH2-groups in TREN. All these findings consolidate the conclusion that our extractive agents have been successfully included in the polymeric PVA matrix.

Characterization of the Elaborated Membranes by SEM

The morphology surfaces of the PVA, PVA-EDTA, PVA-NTA and PVA-TREN membranes were explored by (Scanning Electron Microscopy) SEM and are presented in the Fig. 3a–d. The micrographs show that upon incorporation

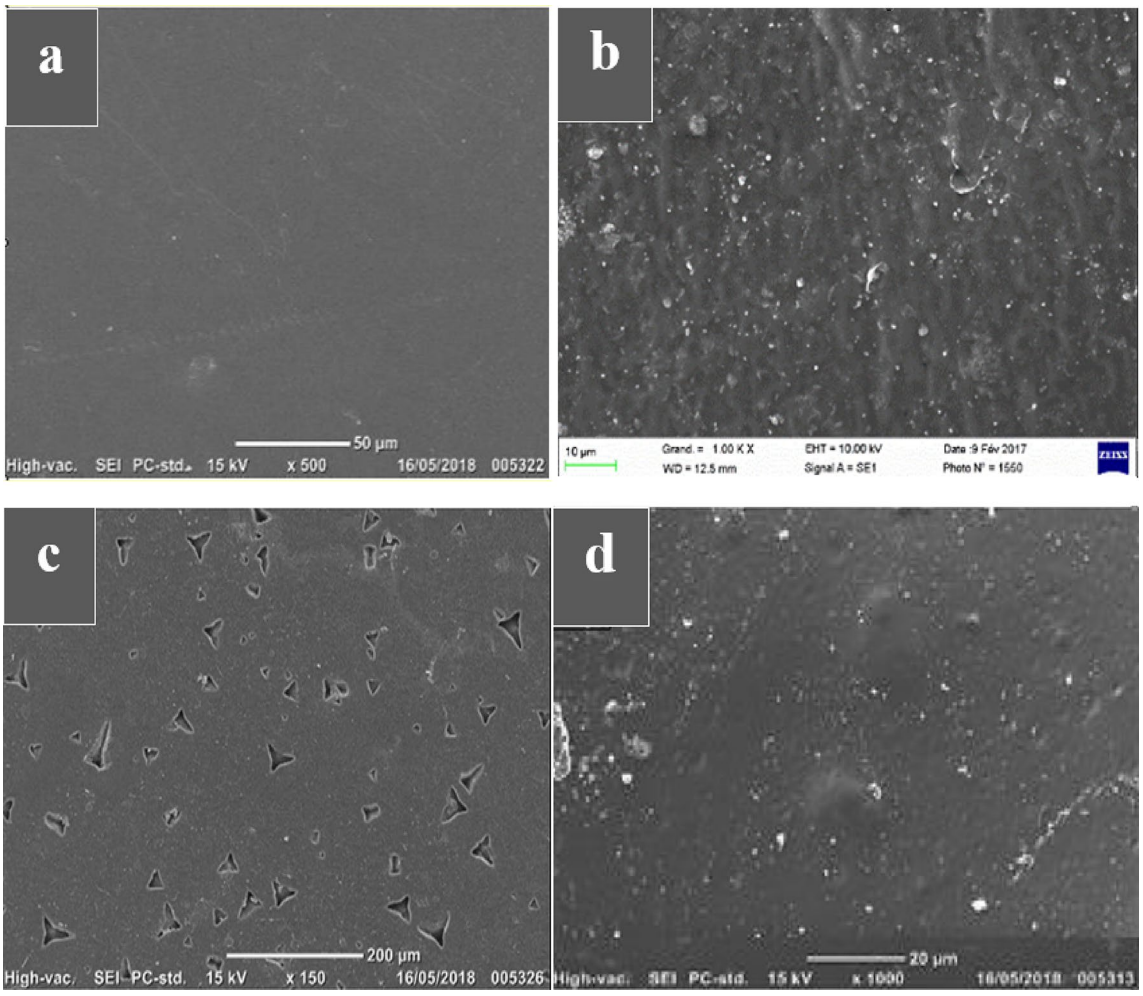

Fig. 3 SEM; **a** PVA support alone, **b** PVA-EDTA, **c** PVA-NTA and **d** PVA-TREN

of the extractive agents into the matrix of the PVA support, the membranes surfaces obtained have become smoother and more porous than the PVA support membrane alone. This result confirms that the extractive agents and the PVA matrix have intermolecular interactions via hydrogen bonds, resulting in the formation of a larger number of crystal-phase PVA [37].For the PVA-EDTA membrane Fig. 3b, the surface is more porous than the other two membranes, which is certainly due to the outward orientation of the hydrophilic nitrogen groups of the EDTA agent.

Effect of the Nature of the Extractive Agent and the Initial Concentration (C_0) the Substrate Nickel (II) Ions

The extractive agent (carrier) is the main component of a polymeric affinity membrane for the oriented processes of transport and facilitated extraction from substrates (metal ions or organic compounds). This element must have an appropriate structure with groups capable of interacting in a targeted manner with the extracted substrates. Therefore the nature and the chemical structure of the carrier are the most important factors to ensure efficient and selective facilitated transport of the substrates through the adopted membranes [38, 39]. Studies of the nature and the chemical structure of the extractive agent on the evolution of the facilitated transport processes of Nickel (II) ions through the PVA-NTA, PVA-EDTA and PVA-TREN membranes have been carried out. The experiments were conducted under the following conditions: **pH** 1, **T** = 298 K, initial concentrations of Nickel (II) ions ranging from 0.200 M, 0.100 M, 0.050 M to 0.025, extractive agents used: NTA, EDTA and TREN, polymer matrix: PVA; solvent/non-solvent: DMSO/water). The technique of UV–visible spectrophotometry made it possible to quantify the evolution of the absorbance of the receiving phase as a function of time and to calculate the C_R concentration of the Nickel (II) ions according to Beer Lamber's law and to present the evolution of the kinetic term predicted by the adopted model (Eq. 1) $-\mathrm{Ln}(C_0\text{-}2C_R) = f(t)$ (Fig. 4).

The line segments obtained confirmed the compatibility of the kinetic model developed with the experimental results. From the slopes of these segments of the function $-\mathrm{Ln}\,(C_0 - 2C_R) = f(t)$, we were able to determine the values of the macroscopic parameters $\boldsymbol{P}$ and $\boldsymbol{J_0}$ for the process studied (Table 1).

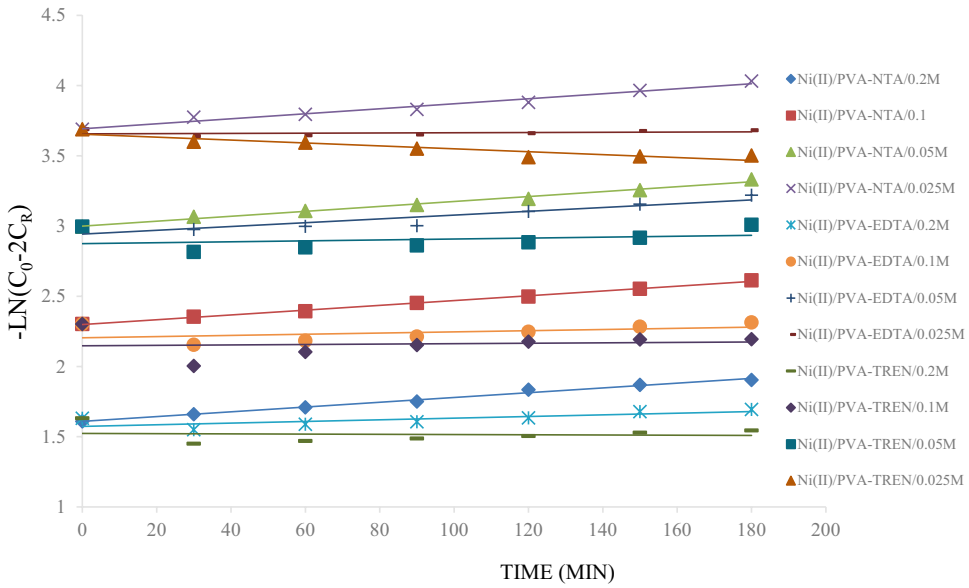

Fig. 4 Representation of the lines $-\ln(C_0\text{-}2C_R) = f(\text{time})$ of the transport of Nickel (II) ions through the three PIMs studied at **pH** = 1 and **T** = 298 K

Table 1 Experimental results for the process of facilitated transport of Nickel (II) ions

Concentration C_0 (M)	PVA-NTA		PVA-EDTA		PVA-TREN	
	$P*10^7$ cm^2 /s	J_0*10^5 mmol/s.cm^2	$P*10^7$ cm^2 /s	J_0*10^5 mmol/s.cm^2	$P*10^7$ cm^2 /s	J_0*10^5 mmol/s.cm^2
0.200	28.12	4.65	16.69	2.76	15.81	2.61
0.100	28.21	2.33	17.19	1.42	16.30	1.35
0.050	28.36	1.17	17.85	0.74	16.51	0.68
0.025	28.41	0.59	18.31	0.38	17.67	036

The results illustrated in Fig. 4 show a linear evolution which confirms the validity of the kinetic model, with the substrate diffusion through the membrane phase as the kinetically determining step. For the same type of membrane (PIM) and the same polymer support (PVA), the values of the parameters $\boldsymbol{P}$ and $\boldsymbol{J_0}$ associated with the membranes performance depend on the chemical nature of the used extractive agent, hence the importance of the choice of the carrier agent, as well as the initial concentration of substrate to improve the properties, the efficiency and the performance of this type of PIMs [40–42].The analysis of these results indicates that the membrane with the NTA extractive agent with three carboxylic groups and a tertiary amine exhibits the highest permeability and initial flux for this oriented processes of facilitated extraction and transport of Nickel (II) ions compared to its counterparts with EDTA and TREN agents. For the three examined membranes, an increase in the substrate initial concentration ($\mathbf{C_0}$) leads to a decrease in $\boldsymbol{P}$ permeability parameter, while an increase in the flux $\boldsymbol{J_0}$. In order to establish more correct interpretations and comparisons on the performance of each membrane adopted, we examined the evolution of the microscopic parameters, $\boldsymbol{K_{ass}}$ and $\boldsymbol{D^*}$, linked to the association of Nickel (II) ions with the semi-mobile sites of the extractive agents in the membrane phases during their diffusion through these organic phases [43, 44]. The Lineweaver–Burk representation $1/\boldsymbol{J_0} = f(1/\mathbf{C_0})$ predicted by the thermodynamic model (Eq. (3)) indicates linear segments shown in Fig. 5. with positive slopes, which helps to confirm the validity of the proposed thermodynamic model, and the establishment of interactions between the Nickel (II) ions and the extractive agents with the formation of a pseudo-entity of composition (1/1), during the diffusion of the Nickel (II) ions at the membrane phase of each of the adopted PIM membranes. From the slopes and the ordinates at the origin of these straight lines, we were able to calculate the values of $\boldsymbol{K_{ass}}$ and $\boldsymbol{D^*}$ according to the expressions of Eq. (4). The values indicated in Fig. 6, for these parameters

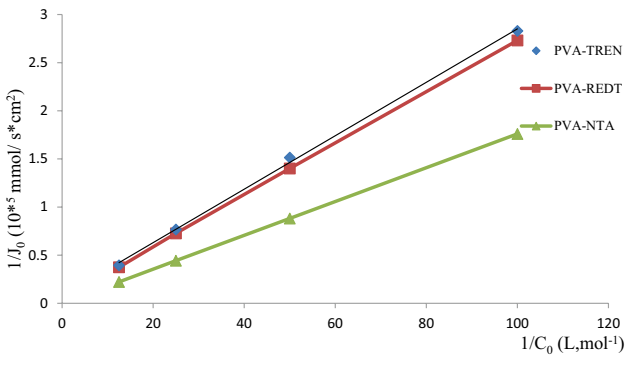

Fig. 5 The Lineweaver–Burk representation for the facilitated transport of Nickel(II) ions through the three membranes (PIM(1), PIM(2), PIM(3))

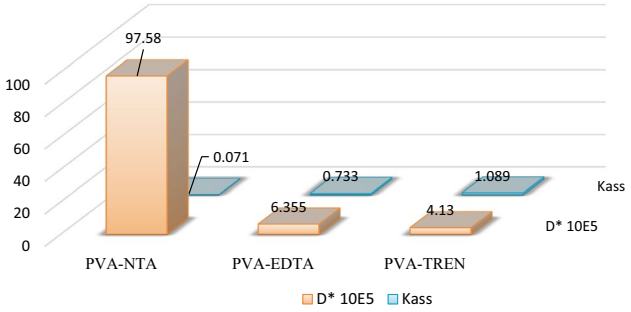

Fig. 6 Graphic representation of the evolution of the $\mathbf{D^*}$ and $\mathbf{K_{ass}}$ microscopic parameters related to the facilitated extraction of Nickel (II) ions by the three PIMs studies

and their evolution are specific for each extractive agent and vary in opposite direction with respect to each other.

The analysis of the results grouped in Fig. 6, confirms that for equal numbers of moles in transporters, the PVA-NTA membrane is the most efficient than its counterpart PIMs PVA -TREN/EDTA for the processes of the extraction and transport of Nickel (II) ions. This result is also well justified by the values of the $\boldsymbol{K_{ass}}$ and confirms that these $\boldsymbol{D^*}$ and $\boldsymbol{K_{ass}}$ parameters are specific to the type of membrane adopted, to the substrate transported and to the nature of the used extractive agent [45–47]. Indeed, the experimental results for $\boldsymbol{P}$ and $\boldsymbol{J_0}$ indicate that the PVA-NTA membrane is more efficient for the facilitated transport of Nickel (II) ions, in agreement with the values of the $\boldsymbol{K_{ass}}$ and $\boldsymbol{D^*}$ parameters, with a high value of the $\boldsymbol{D^*}$ and a low value of the $\boldsymbol{K_{ass}}$. This result is certainly linked to the NTA structure which presents sites of interaction with unfavorable orientations and which interacts with Nickel (II) ions to form pseudo-entities (Nickel(II)-AT) which are not very stable and easily dissociated than their counterparts EDTA and TREN.

Analysis of the Influence of the Temperature Factor

The influence of the temperature factor on the evolution of different parameters related to the facilitated extraction phenomenon on of the Nickel (II) substrate through the three PIMs are of paramount importance in order to explain the performance of these membranes, and to elucidate the mechanisms related to this extraction processes across the adopted membranes. To examine this influence of this parameter, several experiments were conducted at the optimal acidity found (**pH** 1) and at three temperatures 298, 303 and 308 K. The kinetic law $-\mathrm{Ln}(C_0 - 2C_R) = f(t)$, for these experimental results, allow to identify the values of the parameters $\boldsymbol{P}$ and $\boldsymbol{J_0}$ for the three temperatures studied. Table 2, summarizes the values obtained of these parameters.

This data indicates a clear improvement of macroscopic $\boldsymbol{P}$ and $\boldsymbol{J_0}$ parameters as a function of the temperature factor

Table 2 Evolution of **P** and $\mathbf{J_0}$ parameters according to temperature factor for the facilitated extraction process of Nickel (II) ions substrate through elaborated membranes

T (K)	C_0 (M)	PVA-NTA		PVA-EDTA		PVA-TREN	
		$P\times10^7$ ($cm^2\ s^{-1}$)	$J_0\times10^5$ (mmol $cm^{-2}\ s^{-1}$)	$P\times10^7$ ($cm^2\ s^{-1}$)	$J_0\times10^5$ (mmol $cm^{-2}\ s^{-1}$)	$P\times10^7$ ($cm^2\ s^{-1}$)	$J_0\times10^5$ (mmol $cm^{-2}\ s^{-1}$)
298	0.200	28.12	4.65	16.69	2.76	15.81	2.61
	0.100	28.21	2.33	17.19	1.42	16.30	1.35
	0.050	28.36	1.17	17.85	0.74	16.51	0.68
	0.025	28.41	0.59	18.31	0.38	17.67	0.36
303	0.200	28.42	4.69	16.78	2.77	15.93	2.63
	0.100	28.68	2.37	17.27	1.43	16.4	1.35
	0.050	28.96	1.19	17.94	0.74	16.65	0.69
	0.025	29.21	0.60	18.53	0.38	17.81	0.36
308	0.200	28.63	4.73	16.97	2.81	16.12	2.66
	0.100	28.74	2.37	17.36	1.43	16.63	1.37
	0.050	29.16	1.21	18.14	0.75	16.82	0.69
	0.025	29.43	0.61	18.74	0.39	17.95	0.38

and show that an increase of this important factor leads to an improvement of the membrane performance. In the temperature interval studied from 298 to 308 K, a better evolution of $\boldsymbol{P}$ and $\boldsymbol{J_0}$ parameters for the adopted membranes (PVA-EDTA and PVA-TREN), while for PVA-NTA membrane the performances are higher at the analyzed temperatures. To understand and to interpret these results and determine the movement nature of the substrate **S** through the membrane phase, it is necessary to study the effect of temperature factor on the evolution of microscopic parameters $\boldsymbol{K_{ass}}$ and $\boldsymbol{D^*}$. Based on the Lineweaver–Burk representation of the function $1/\boldsymbol{J_0} = f\,(1/\mathbf{C_0})$ (Eq. (3)), the line shown by the graph in the following figure can be exploited to obtain the values of these specific parameters (Fig. 7).

The slopes and intercepts of these line segments are used according to the terms of (Eq. (4)) to determine the values of the parameters $\boldsymbol{K_{ass}}$ and $\boldsymbol{D^*}$. The values calculated for these microscopic parameters at the three temperatures studied are summarized in the table below (Table 3).

According to the results obtained grouped in Table 3, we observe a clear influence of the temperature factor on the evolution of the microscopic parameters. When the temperature of the medium increases, the apparent diffusion coefficient $\boldsymbol{D^*}$ of the Nickel (II) ions increases, while the association constant $\boldsymbol{K_{ass}}$ of these ions with each of the transporting agents decreases. Consequently, this evolution explains the better performance of the membranes adopted at high temperature. The analysis of all the results clearly shows that the PIM membrane prepared based on the transporter agent NTA is the most efficient, because it allows to obtain the best values of permeabilities $\boldsymbol{(P)}$ and initial fluxes $(\boldsymbol{J_0})$ as well as high values of the coefficient $\boldsymbol{D^*}$ which correspond to low values of the $\boldsymbol{K_{ass}}$ constant for these facilitated transport processes of Nickel (II) ions. The PIM membrane prepared based on the extractive agent EDTA (PVA-EDTA) comes in second position in terms of performance, followed by the PIM membrane prepared based on the agent TREN. All these membranes were successfully used for the first time for these oriented processes of facilitated- transport and extraction of Nickel (II) ions.

On the other hand, an increase in the temperature factor leads to a decrease in the stability of the substrate-extractant (ST) entity, and a rapid dissociation. This significant result shows that the movement of the substrate (S) through the organic membrane phase is based on its interaction with the extractive agent (T) in opposite reactions (association/dissociation) whose rates increase with temperature. Thus, the passage of the Nickel (II) substrate through the membrane phase is an apparent movement of diffusion, by successive jumps of the molecules of the substrate from one site to another of the extracting agent. (Fig. 8).

To confirm these results and elucidate the real mechanism related to the process studied through each type of adopted membrane, we determined the values of the activation and the thermodynamic parameters $\boldsymbol{(E_a, \Delta H^{\#}_{ass}, \Delta S^{\#}, \Delta H^{\#}_{diss}}$ and $\boldsymbol{\Delta H_{th})}$ for the transition state of the diffusion step of the substrate through the membrane phase (rate-determining step). For this, we have examined the evolution of $\boldsymbol{J_0}$ and $\boldsymbol{K_{ass}}$ values with temperature factor according to Arrhenius [$\mathrm{Ln}\,(\boldsymbol{J_{0moy}}) = f\,(1/T)$] and Van't Hof [$\mathrm{Ln}\,(\boldsymbol{K_{ass}}) = f(1/T)$] relationships (Eqs. 6 and 9). The values of the slopes and intercepts of the straight segments obtained were used to determine the values of the parameters of $\boldsymbol{E_a}$ and $\boldsymbol{Aj}$ so that the values of the activation thermodynamic parameters were determined at 298 K according to the expressions in Eqs. 7, 8 and 10). All obtained data is presented in Table 4.

The results in Table 4, indicate the values of a low and close energy parameters. These parameters are relative to

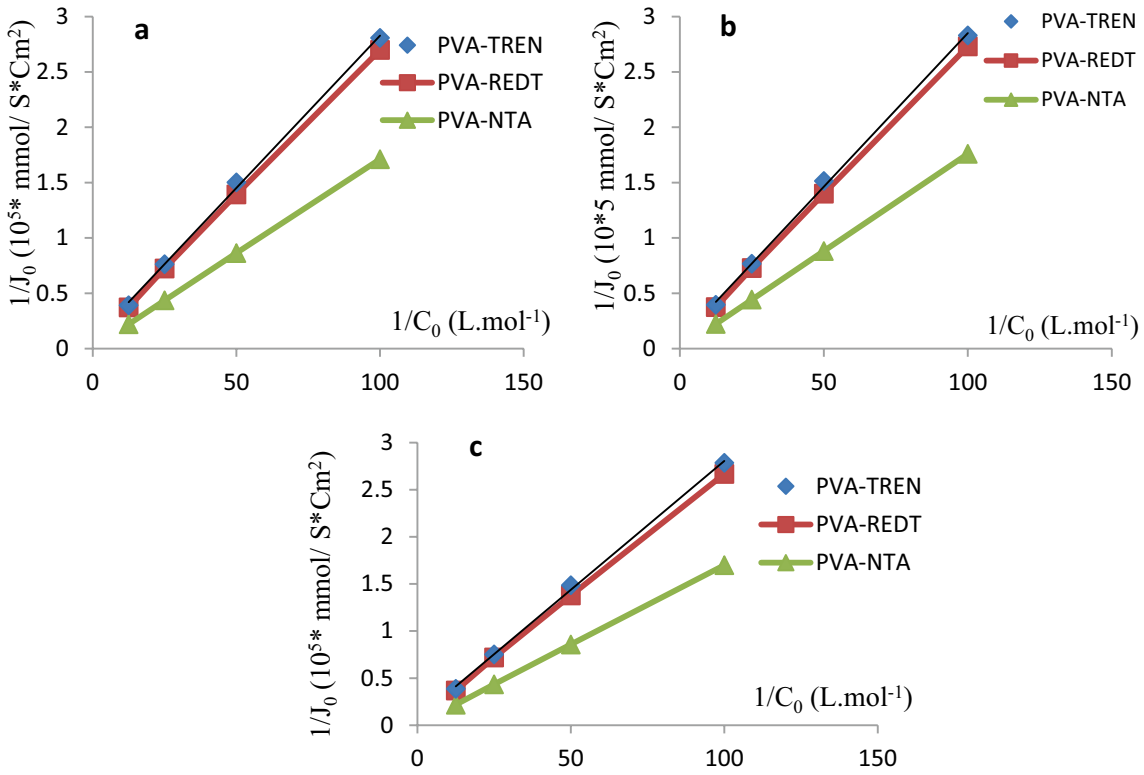

Fig. 7 Lineweaver–Burk representations [$1/J_0 = f(1/C_0)$] for facilitated extraction process of Nickel (II) ions substrate across the adopted membranes at studied temperature (**a** = 298 K, **b** = 303 K and **c** = 308 K)

Table 3 Influence of temperature factor on the evolution of $\mathbf{K_{ass}}$ and **D*** parameters to facilitated extraction process of Nickel (II) ions substrate through the adopted membranes

T (K)	PVA-NTA		PVA-EDTA		PVA-TREN	
	$D^* \times 10^5$ ($cm^2\ s^{-1}$)	K_{ass}	$D^* \times 10^5$ ($cm^2\ s^{-1}$)	K_{ass}	$D^* \times 10^5$ ($cm^2\ s^{-1}$)	K_{ass}
298	97.580	0.071	6.355	0.073	4.136	1.089
303	103.421	0.068	8.751	0.061	7.563	0.975
308	109.254	0.052	12.035	0.049	9.786	0.753

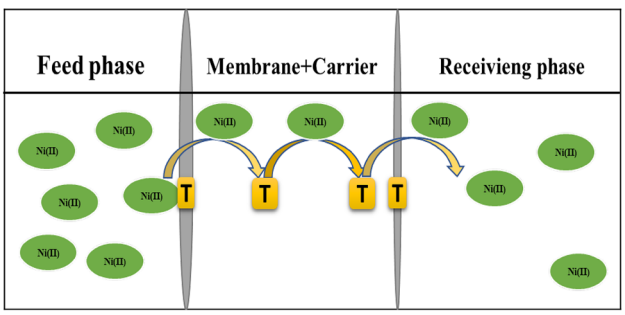

Fig. 8 Apparent diffusion movement of the substrate by successive jumps from one site to another of the extractive agent across the membrane organic phase

the transition state of the rate-determining step, and the negative values of the parameter $\Delta S^{\#}$ confirm that in the transition state there is an association of Nickel (II) ions with the extractive agents sites. The interaction of each agent adopted, to form an entity (Nickel (II)-AT) whose structure is a function of the nature and structure of the interaction site of the extractive agent AT [46, 48]. However, the negative values are very close to the entropy of activation parameter ($\Delta S^{\neq}$) for the transition states of the entities (Nickel (II)-AT) formed with the agents NTA and EDTA (-288.43 and -251.75 J/mol.K) indicating for the mechanisms of the processes reflects late transition states, whose structures are close and with similar bidentate chelation sites. Whereas,

Table 4 Evolution of activation and the thermodynamic parameters for the facilitated extraction-oriented process of Ni (II) ions through membrane types: PVA-NTA, PVA-EDTA and PVA-TREN

PIMs	E_a (kJ/mol)	$\Delta S^{\#}$(J/mol.K)	$\Delta H^{\#}_{ass}$ (kJ/mol)	ΔH_{th} (kJ/mol)	$\Delta H^{\#}_{diss}$ (kJ/mol)
PVA-NTA	11.25	− 288.43	16.15	− 19.83	36.33
PVA- EDTA	17.46	− 251..75	23.18	− 21.73	44.91
PVA-TREN	25.73	− 243.86	24.19	− 26.23	50.42

the transition state for the entity (Nickel (II)-TREN) which is also late, whose value of $\Delta S^{\neq}$ is less negative (-243.86 J/mol.K), indicates that this transition state whose structure is less ordered and different from those of NTA and EDTA and which also corresponds to a bidentate chelation site. The low values of the activation and thermodynamic parameters ($\boldsymbol{E_a}$, $\boldsymbol{\Delta H^{\#}_{ass}}$, $\boldsymbol{\Delta S^{\#}}$, $\boldsymbol{\Delta H^{\#}_{dis}}$ and $\boldsymbol{\Delta H_{th}}$) explain the good performances of described membranes and make it possible to explain the difference between these performances, especially for the PVA-TREN membrane whose values of parameters $\boldsymbol{\Delta H^{\#}_{ass}}$ and $\boldsymbol{\Delta H^{\#}_{dis}}$ are the highest (Table 4), explain its weaker performance. This difference in performance certainly lies in the number of favorable orientations of chelation sites which is low in the case of the PVA-TREN membrane [49, 50]. In addition, the difference between the values of this important parameter $\boldsymbol{\Delta H^{\#}_{diss}}$, perfectly explains the order of observed performances for the adopted membranes.

Conclusion

For this study, we prepared three affinity membranes namely PVA-NTA, PVA-EDTA and PVA-TREN intended for the oriented processes of the facilitated extraction and recovery of Nickel (II) ions from Li-ion battery waste. These membranes contain chelating compounds as extractive agents or carriers including NTA, EDTA and TREN. The characterization methods verified the inclusion or the functionalization of PVA polymer support by the carrier transporting agents, to develop the three elaborated membranes. Experiments relating to oriented processes of transport and extraction, showed that the presence of carboxylic and amine groups in the membrane phases led to a significant improvement in the membrane transport efficiency of Nickel (II) ions through theses phases. Then we studied the influence of two factors on the extraction phenomenon, in particular, the carrier agent chemical nature and the concentration of substrate in the medium. Macroscopic (permeability $\boldsymbol{P}$ and initial flux $\boldsymbol{J_0}$) and microscopic (apparent diffusion coefficient $\boldsymbol{D^*}$ and the association constant $\boldsymbol{K_{ass}}$) parameters have been quantified. Finally, the important studies on the influence of temperature factor have also made it possible to determine the activation and thermodynamic parameters ($\boldsymbol{E_a}$, $\boldsymbol{\Delta H^{\#}_{ass}}$, $\boldsymbol{\Delta S^{\#}}$, $\boldsymbol{\Delta H^{\#}_{dis}}$ and $\boldsymbol{\Delta H_{th}}$) for the transition state of the rate-determining step (diffusion of the substrate through the membrane phase), related to the mechanism of studied process. The original values of these parameters allow two main interpretations: firstly, the process studied is a process much more oriented by the structures of substrate and extractive agent, and not by the energy of the reaction medium. The second interpretation is very important: the structure of the unstable intermediate entity (ST) necessary for the migration of the substrate through the membrane phase is the same whatever the type of membrane adopted. The oriented processes of the facilitated extraction of Nickel (II) ions through the three examined membranes, made it possible to compare their performances in order to determine the optimal experimental and structural conditions for the realization of these facilitated transport processes through these different developed membranes. Thus, the results show that the interaction sites of the NTA agent in the PVA polymer matrix are more favorable for transporting Nickel (II) ions through the membrane phase, therefore this membrane shows a better performance as compared to its counterparts with TREN and EDTA extractive agents.

Acknowledgements The work of this manuscript was carried out within the framework of the PPR2 project, which is financed by the Ministry of Higher Education, Scientific Research and Executive Training (MESRSFC) and the National Center for Research in Science and Technology (CNRST). We would like to thank these two organizations for their financial support.

Authors Contributions HZ: conceptualization, methodology and experimental manipulations, YC: Collection and preparation of samples. MR: collection and preparation of samples. OK: realization of FTIR spectra. SM: discussion and argumentation of the results. KT: discussion and argumentation of the results. LL: SEM micrographs, interpretation (cooperation). MH: writing—formatting and general discussion.

Declarations

Competing interest The authors declare that they have no known competing financial interests or personal relationships that could have appeared to influence the work reported in this paper.

Ethical Approval Not applicable.

Consent to Participate Not applicable.

References

1. Li L, Ge J, Wu F et al (2010) Recovery of cobalt and lithium from spent lithium ion batteries using organic citric acid as leachant. J Hazard Mater 176:288–293. https://doi.org/10.1016/j.jhazmat.2009.11.026
2. Gaines L, Richa K, Spangenberger J (2018) Key issues for Li-ion battery recycling. MRS Energy Sustain 5:1–14. https://doi.org/10.1557/mre.2018.13
3. Wang X, Gaustad G, Babbitt CW et al (2014) Economic and environmental characterization of an evolving Li-ion battery waste stream. J Environ Manag 135:126–134. https://doi.org/10.1016/j.jenvman.2014.01.021
4. Wang X, Gaustad G, Babbitt CW (2016) Targeting high value metals in lithium-ion battery recycling via shredding and size-based separation. Waste Manag 51:204–213. https://doi.org/10.1016/j.wasman.2015.10.026
5. Richa K, Babbitt CW, Gaustad G, Wang X (2014) A future perspective on lithium-ion battery waste flows from electric vehicles. Resour Conserv Recycl 83:63–76. https://doi.org/10.1016/j.resconrec.2013.11.008
6. Sethurajan M, Gaydardzhiev S (2021) Bioprocessing of spent lithium ion batteries for critical metals recovery—a review. Resour Conserv Recycl 165:105225. https://doi.org/10.1016/j.resconrec.2020.105225
7. Notter DA, Gauch M, Widmer R et al (2010) Erratum: Contribution of li-ion batteries to the environmental impact of electric vehicles (Environmental Science & Technology (2010) 44 (6550–6556)). Environ Sci Technol 44:7744. https://doi.org/10.1021/es1029156
8. Zeng X, Li J, Liu L (2015) Solving spent lithium-ion battery problems in China: opportunities and challenges. Renew Sustain Energy Rev 52:1759–1767. https://doi.org/10.1016/j.rser.2015.08.014
9. Mulvaney D, Richards RM, Bazilian MD et al (2021) Progress towards a circular economy in materials to decarbonize electricity and mobility. Renew Sustain Energy Rev 137:110604. https://doi.org/10.1016/j.rser.2020.110604
10. Mossali E, Picone N, Gentilini L et al (2020) Lithium-ion batteries towards circular economy: a literature review of opportunities and issues of recycling treatments. J Environ Manag. https://doi.org/10.1016/j.jenvman.2020.110500
11. Sinha V, Patel MR, Patel JV (2010) Pet waste management by chemical recycling: a review. J Polym Environ 18:8–25. https://doi.org/10.1007/s10924-008-0106-7
12. Schwich L, Küpers M, Finsterbusch M et al (2020) Recycling strategies for ceramic all-solid-state batteries—part I: study on possible treatments in contrast to li-ion battery recycling. Metals (Basel) 10:1–19. https://doi.org/10.3390/met10111523
13. Liu C, Lin J, Cao H et al (2019) Recycling of spent lithium-ion batteries in view of lithium recovery: a critical review. J Clean Prod 228:801–813. https://doi.org/10.1016/j.jclepro.2019.04.304
14. Makuza B, Tian Q, Guo X et al (2021) Pyrometallurgical options for recycling spent lithium-ion batteries: a comprehensive review. J Power Sources 491:229622. https://doi.org/10.1016/j.jpowsour.2021.229622
15. Zhang L Review of current progress of recycling technologies for metals from waste electrical and electronic equipment, Xu Z (2016) A review of current progress of recycling technologies for metals from waste electrical and electronic equipment. J Clean Prod 127:19–36. https://doi.org/10.1016/j.jclepro.2016.04.004
16. Asadi Dalini E, Karimi G, Zandevakili S, Goodarzi M (2020) A review on environmental, economic and hydrometallurgical processes of recycling spent lithium-ion batteries. Miner Process Extr Metall Rev 00:1–22. https://doi.org/10.1080/08827508.2020.1781628
17. Silvestre CIC, Santos JLM, Lima JLFC, Zagatto EAG (2009) Liquid-liquid extraction in flow analysis: a critical review. Anal Chim Acta 652:54–65. https://doi.org/10.1016/j.aca.2009.05.042
18. Mahanty B, Mohapatra PK, Leoncini A, Verboom W (2022) Liquid – liquid extraction and supported liquid membrane transport of neptunium (IV) across a flat-sheet supported liquid membrane containing a TREN-DGA derivative liquid – liquid extraction and supported liquid membrane transport of neptunium (IV) Ac. Solvent Extr Ion Exch 00:1–25. https://doi.org/10.1080/07366299.2022.2074501
19. Lei Y, Zhan Z, Saakes M et al (2021) Electrochemical recovery of phosphorus from acidic cheese wastewater: feasibility, quality of products, and comparison with chemical precipitation. ACS ES&T Water 1:1002–1013. https://doi.org/10.1021/acsestwater.0c00263
20. (2020) Version of Record: https://www.sciencedirect.com/science/article/pii/S0043135420312823
21. Tohamy HAS, El-Sakhawy M, Kamel S (2021) Carboxymethyl cellulose-grafted graphene oxide/polyethylene glycol for efficient Ni(II) adsorption. J Polym Environ 29:859–870. https://doi.org/10.1007/s10924-020-01920-7
22. Huang R, Zhang Q, Yao H et al (2021) Ion-exchange resins for efficient removal of colorants in bis(hydroxyethyl) terephthalate. ACS Omega 6:12351–12360. https://doi.org/10.1021/acsomega.1c01477
23. Touarssi I, Oukkass S, Habibi Z et al (2021) Tris 2-aminoethyl amine (TREN) agent to quantify interaction and extraction capacity of VO2+ions for oriented membrane processes. Mater Today Proc 45:7711–7717. https://doi.org/10.1016/j.matpr.2021.03.334
24. Chaouqi Y, Ouchn R, Eljaddi T et al (2019) Tris 2-aminoethyl amine (TREN) agent to quantify interaction and extraction capacity of VO2+ions for oriented membrane processes. Mater Today Proc 13:698–705. https://doi.org/10.1016/j.matpr.2019.04.030
25. El Atmani EH, Benelyamani A, Mouadili H et al (2018) The oriented processes for extraction and recovery of paracetamol compound across different affinity polymer membranes. Parameters and mechanisms. Eur J Pharm Biopharm 126:201–210. https://doi.org/10.1016/j.ejpb.2017.06.001
26. Hassoune H, Rhlalou T, Verchère JF (2009) Mechanism of transport of sugars across a supported liquid membrane using methyl cholate as mobile carrier. Desalination 242:84–95. https://doi.org/10.1016/j.desal.2008.03.033
27. Touarssi I, Mourtah I, Chaouqi Y et al (2019) Conceptualization and quantification of oriented membrane processes for recovering vanadium ions from acidic industrial discharges. J Environ Chem Eng. https://doi.org/10.1016/j.jece.2019.103182
28. T E, (2015) New supported liquid membrane for studying facilitated transport of U(VI) ions using tributyl phosphate (TBP) and tri-n-octylamine (TOA) as carriers from acid medium. BAOJ Chem. https://doi.org/10.24947/baojc/1/1/103
29. Kamal O, Eljaddi T, El Atmani EH et al (2017) Process of facilitated extraction of vanadium ions through supported liquid membranes: parameters and mechanism. Adv Mater Sci Eng. https://doi.org/10.1155/2017/3425419
30. Tarhouchi S, Louafy R, Houssine E et al (2021) Kinetic control concept for the diffusion processes of Paracetamol active molecules across affinity polymer membranes. BMC Chem 16(1):1–17
31. Hlaïbi M, Tbeur N, Benjjar A et al (2011) Carbohydrate-resorcinarene complexes involved in the facilitated transport of alditols across a supported liquid membrane. J Membr Sci 377:231–240. https://doi.org/10.1016/j.memsci.2011.04.055
32. Benjjar A, Eljaddi T, Kamal O et al (2014) The development of new supported liquid membranes (SLMs) with agents: methyl

cholate and resorcinarene as carriers for the removal of dichromate ions (Cr2O72-). J Environ Chem Eng 2:503–509. https://doi.org/10.1016/j.jece.2013.10.003
33. Amini M, Rahbar-Kelishami A, Alipour M, Vahidi O (2018) Technique of supported liquid membranes (SLMs) for the facilitated transport of vanadium ions (VO2+). Parameters and mechanism on the transport process. J Membr Sci Res 4:121–135. https://doi.org/10.22079/JMSR.2017.63968.1138
34. Touaj K, Tbeur N, Hor M, Verchère JF, Hlaïbi M (2009) A supported liquid membrane (SLM) with resorcinarene for facilitated transport of methyl glycopyranosides: parameters and mechanism relating to the transport. J Membr Sci 337(1–2):28–38
35. Chaouqi Y, El Bouchti M, Ouchn R et al (2020) Oriented membranes processes for facilitated extraction and recovery of some industrial dyes across polymer inclusion membranes containing Chitin as new extractive agent. IOP Conf Ser Mater Sci Eng. https://doi.org/10.1088/1757-899X/827/1/012001
36. Zhang J, Xu WR, Zhang YC et al (2020) In situ generated silica reinforced polyvinyl alcohol/liquefied chitin biodegradable films for food packaging. Carbohydr Polym 238:116182. https://doi.org/10.1016/j.carbpol.2020.116182
37. Bolto B, Zhang J, Wu X, Xie Z (2020) A review on current development of membranes for oil removal from wastewaters. Membranes (Basel) 10:1–18. https://doi.org/10.3390/membranes10040065
38. Drew D, North RA, Nagarathinam K, Tanabe M (2021) Structures and general transport mechanisms by the major facilitator superfamily (MFS). Chem Rev 121:5289–5335. https://doi.org/10.1021/acs.chemrev.0c00983
39. Eljaddi T, Lebrun L, Hlaibi M (2017) Review on mechanism of facilitated transport on liquid membranes. J Membr Sci Res 3:199–208. https://doi.org/10.22079/jmsr.2017.50137.1110
40. Kamal O, Eljaddi T, Atmani EHEL et al (2017) Grafted polymer membranes with extractive agents for the extraction process of VO2+ ions. Polym Adv Technol 28:541–548. https://doi.org/10.1002/pat.3955
41. Mourtah I, Touarssi I, Chaouqi Y et al (2019) Membrane oriented processes for elimination and recovery of Cr(VI) and Cr(III) through a grafted polymer membrane. Mater Today Proc 13:1039–1048. https://doi.org/10.1016/j.matpr.2019.04.069
42. Tbeur N, Rhlalou T, Hlaíbi M et al (2000) Molecular recognition of carbohydrates by a resorcinarene. Selective transport of alditols through a supported liquid membrane. Carbohydr Res 329:409–422. https://doi.org/10.1016/S0008-6215(00)00188-9
43. Mouadili H, Majid S, Kamal O et al (2018) New grafted polymer membrane for extraction, separation and recovery processes of sucrose, glucose and fructose from the sugar industry discharges. Sep Purif Technol 200:230–241. https://doi.org/10.1016/j.seppur.2017.12.012
44. Chaouqi Y, Ouchn R, Eljaddi T et al (2019) New polymer inclusion membrane containing NTA as carrier for the recovery of chromium and nickel from textiles wastewater. Mater Today Proc 13:698–705. https://doi.org/10.1016/j.matpr.2019.04.030
45. Louafy R, Benelyamani A, Tarhouchi S et al (2020) Parameters and mechanism of membrane-oriented processes for the facilitated extraction and recovery of norfloxacin active compound. Environ Sci Pollut Res 27:37572–37580. https://doi.org/10.1007/s11356-020-09311-0
46. Hor M, Riad A, Benjjar A et al (2010) Technique of supported liquid membranes (SLMs) for the facilitated transport of vanadium ions (VO2+). Parameters and mechanism on the transport process. Desalination 255:188–195. https://doi.org/10.1016/j.desal.2009.12.023
47. Benjjar A, Eljaddi T, Kamal O et al (2013) Membrane oriented processes for elimination and recovery of Cr(VI) and Cr(III) through a grafted polymer membrane. Open J Phys Chem 03:103–114. https://doi.org/10.4236/ojpc.2013.33013
48. Hassoune H, Rhlalou T, Verchère JF (2008) Studies on sugars extraction across a supported liquid membrane: complexation site of glucose and galactose with methyl cholate. J Membr Sci 315:180–186. https://doi.org/10.1016/j.memsci.2008.02.021
49. Fuoco A, Galier S, Roux-de Balmann H, De Luca G (2015) Correlation between macroscopic sugar transfer and nanoscale interactions in cation exchange membranes. J Membr Sci 493:311–320. https://doi.org/10.1016/j.memsci.2015.06.028
50. Harayama T, Riezman H (2018) Understanding the diversity of membrane lipid composition. Nat Rev Mol Cell Biol 19:281–296. https://doi.org/10.1038/nrm.2017.138